
Article:
Lu, P., Lewis, S.R., Fretwell-Smith, S. et al. (2 more authors) (2019) Laser cladding of rail; the effects of depositing material on lower rail grades. Wear, 438-439. 203045. ISSN 0043-1648

https://doi.org/10.1016/j.wear.2019.203045

LASER CLADDING OF RAIL; THE EFFECTS OF DEPOSITING MATERIAL ON LOWER RAIL GRADES

P Lu [1], S R Lewis [2], S Fretwell-Smith [2], DI Fletcher [1], R Lewis [1,*]

[1] Department of Mechanical Engineering, University of Sheffield, Mappin Street, Sheffield, S1 3JD, UK
[2] British Steel, Brigg Road, Scunthorpe, Lincolnshire, DN16 1XA, UK

[*] E-mail: roger.lewis@sheffield.ac.uk

Abstract: This paper presents a study comparing the wear performance of laser clad rails. A grade of martensitic stainless steel (MSS) was deposited on two substrate materials: The Europe standard rail steel R260, and a lower grade rail steel R200. A twin-disc method has been used to simulate the contact of wheel and rail under closely controlled conditions. Although cladding on a lesser grade of rail does have an effect on the hardness and wear performance of the clad layer, the resulting wear performance of the clad layer assessed using this approach is still vastly improved over R260 material alone.

Keywords: laser cladding, wheel/rail contact, wear, microstructure, twin-disc testing.

1. Introduction and Background

A major proportion of a train network operational cost is the rail maintenance. The cost of replacement of the worn rail or improvement of the rail's tribological properties, corrosion properties and contact fatigue resistance, is significant. Meanwhile network downtime caused by rail maintenance also has a great impact on the disruption to commuters and cargo shipping.

Railway rail is rolled from a single grade of steel yet different parts of the rail section require their own operating properties. For example, the rail head requires strong tribological properties while the web and foot are required to be structurally robust. There are two main factors that affect the durability of rail track: wear and rolling contact fatigue (RCF) [1, 2]. Wear and RCF resistant materials are available [3], however, it would be either difficult or costly to manufacture entire rail sections from them. One solution is to use premium grade rail steels which have good wear and RCF resistance. These premium rails are usually heat treated. This procedure is an additional step during the rail manufacturing process and hence has increased cost. Another common method to alleviate RCF, is to periodically grind the rail head which reduces crack development [4]. Other solutions such as surface treatments by peening, case hardening or surface coating can also enhance the wear and RCF performance of many engineering materials. However, rails are usually rolled in lengths of over 100 metres so incorporating these processes into rail manufacture would be impractical and costly. The maximum shear stress, which is a primary driver of RCF, occurs below the surface of the material in most cases. Therefore, traditional surface coatings are not sufficiently thick to prevent damage caused by this sub-surface shear stress. In recent research [5-8], laser cladding technology was shown to be an alternative way to improve the durability of rail both in terms of wear and RCF [7, 8]. Laser cladding technology can deposit a wide range of beneficial materials onto a certain area or an entire existing rail surface. Instead of rolling the entire rail section with costly premium material, laser cladding allows the deposition of the premium material onto the surface of a standard or cheaper structural base steel. Tests performed in [7, 8] show significantly enhanced performance and durability of rail which had been laser clad. In addition, rail not only consists of straight track, but is also made up of other rail constructed components such as switches and crossings (S&C), insulated block joints (IBJs), check rails and tight radius curves. The related maintenance costs of these components are much greater than that of straight track [9, 10]. The laser cladding process offers the possibility to locally treat those components where they are more prone to damage, leading to new enhanced components with potentially reduced overall lifetime costs. Laser cladding offers the opportunity of altering certain surfaces of components and constructions to meet each individual requirement.

As mentioned above, resistance to wear and RCF play two vital roles in the maintenance of a rail network. Anti-wear characteristics are related to the hardness and microstructure of the material, which can be improved with laser cladding technology. For example, Guo et al. [11] investigated the microstructure and tribological properties of a Ni-based coating after laser cladding with Tungsten carbide Nickel (WC–Ni) particles, and they found that the hardness of the conventional alloy coatings is greatly improved due to the formation of a new hard WC phase. Guo et al. [12] proved that the wear rate was dramatically reduced after investigating the microstructure of the laser cladding layer (Co-based alloy) on the rail-wheel or rail surface. Wang et al. [13] investigated the effect of the amount of lanthanum oxide (Fe-based alloy), in a laser cladding deposit and they achieved a more refined microstructure, which had a greater RCF resistance without sacrificing the surface hardness. Research on laser cladding has not only been performed at a scaled model test. Lewis et al. [14] conducted a series of full-scale tests on a rail that had been laser clad with a layer of high performance material. In these tests it was shown that the clad rails

not only had decreased wear rates, but also improved fatigue resistance over standard rail.

It can be seen that wear and RCF resistance of laser clad coatings is becoming an important research issue and the current state of the art focuses on characterising the wear and RCF resistance over a wide range of laser clad materials, such as in [11-13, 15-18].

In contrast to the previous laser cladding research, there is little work in investigating the contribution of the substrate material. When the head of a rail is clad with premium material the requirements of the substrate become purely structural and it becomes shielded from damage at the rail surface. Moreover, the migration of peak sub-surface shear stress towards the rail surface under high rail-wheel traction conditions places this particularly damaging stress into the harder clad layer, rather than the more vulnerable bulk material. This is especially beneficial as cyclic shear stress combined with compressive wheel load is responsible for rail plastic damage accumulation and crack initiation by the ratchetting mechanism. As such, the work described in this paper was intended to investigate the usage of different substrate materials, namely R200 and R260, using the same cladding material. This also provides an insight into how the substrate affects the properties of the cladding layer, dilution zone and overall rail durability.

2. Method and Materials

2.1. Experimental apparatus

The wear experiments were carried out using the Sheffield University ROlling Sliding (SUROS) twin-disc test machine [19]. Fig. 1 shows a schematic of the SUROS rig and typical discs used. This machine uses a line contact between twin-disc specimens to simulate the normal load and rolling-sliding behaviour at the wheel/rail interface. Two discs with diameters of 47 ± 0.2 mm serve as a rail disc (upper specimen) and a wheel disc (lower specimen). These discs are powered and controlled by an AC motor and a Colchester lathe. The difference of speed of wheel and rail discs is used to control the creep. The slip ratio is defined in Eq. 1, where ω and r are the rotational speed and rolling radius of the discs, respectively. The load is applied to the wheel disc by a hydraulic piston and load cell.

$$Slip = \frac{\omega_{wheel} \cdot r_{wheel} - \omega_{rail} \cdot r_{rail}}{\omega_{wheel} \cdot r_{wheel} + \omega_{rail} \cdot r_{rail}} \quad (1)$$

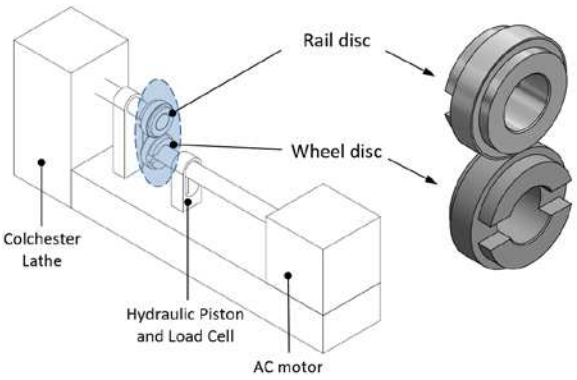

Figure 1 *SUROS machine and samples.*

2.2. Specimens

2.2.1. Sample materials

All the wheel and the rail discs' materials were manufactured from actual wheel and rail. The wheel discs were made from R8 wheel steel, with the properties shown in Table 1.

Table 1 *R8 Steel grades specified by EN.*

Region	Specification	Steel grade	Carbon content	Hardness
			(% by mass)	(HB)
Europe	EN 13262	ER 8	≤ 0.56	258-296

For the rail substrates, two materials were chosen for comparison, R260 and R200, with the properties shown in Table. 2.

Table 2 *R200 and R260 Steel grades specified by EN.*

Region	Specification	Steel grade	Carbon content	Hardness
			(% by mass)	(HB)
Europe	EN 13674-1	R 200	0.4-0.6	200-240
		R 260	0.62-0.8	260-300

The R260 grade material, as the current standard rail material widely used in UK and some other countries in Europe, was chosen to provide representative results for comparison. While the other lower grade steel substrate R200 is still widely used throughout Europe. R200 has some properties which potentially make it an ideal substrate candidate for laser cladding, for instance:

- lower carbon content than R260 (0.4-0.6% compared to 0.62-0.8%) and hence a lower bulk hardness of 200 HB minimum as compared to roughly 260 HB minimum for R260 grade.
- easier machinability, better weld-ability, and lower rates of foot failure [20].

Both rail substrates (R200 and R260) were machined to cylinders with a diameter of 46 ± 0.2 mm, clad and then machined into discs.

2.2.2. Laser cladding

In this study, one-step laser cladding by powder injection was employed to clad the rail cylinder specimens. A grade of martensitic stainless steel (MSS), which was found to be less susceptible to ratchetting due to its high hardness and shear yield strength in previous tribological tests [16], was deposited onto the two different grades of rail material. Fig. 2(a) shows a schematic of this cladding process, where the high energy laser beam is focused on and scanned across the curved surface of the rail substrate. As the MSS powder passes through the laser it is melted and fuses with the melt pool on the surface of the substrate material. The shaft rotates under the laser to allow a single track of clad to be deposited on the surface. Individual tracks are then overlapped side-by-side to cover the shaft surface. As the laser passes the substrate will start to cool at a rapid rate. This high rate of cooling is due to the greater

volume of substrate which is at a lower temperature than the freshly laid deposit. This heating and rapid cooling of the substrate causes changes in its microstructure throughout a certain depth of the bulk, which is called the heat affected zone (HAZ).

Fig. 2 (b) gives an example of the shafts covered by cladding tracks. It should be noted that all the machining parameters including the MSS powder feeding rate, the laser power and the rotating speed of the shaft were all optimized to achieve a poreless clad layer with outstanding mechanical properties, as well as a satisfactory bonding between the substrate and deposit.

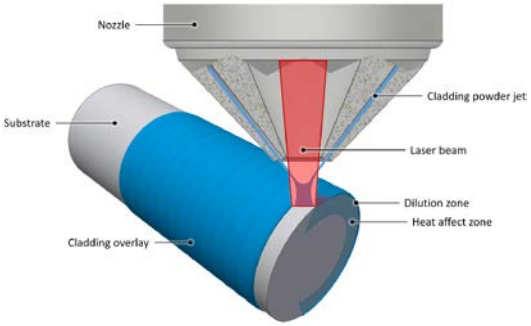

(a)

(b)

Figure 2 *Laser cladding (a) laser cladding scheme (b) laser clad cylinders prior to finish grinding.*

Once cooled the clad layer was ground back to give a smooth surface finish which was suitable for testing. The single layer of MSS material had a mean post-grinding thickness of 1.10 mm. The ground cylinders were then sectioned and machined into SUROS rail specimens with dimensions as shown in Fig. 3. The wheel discs were not clad as the focus of this work was the cladding of rails only.

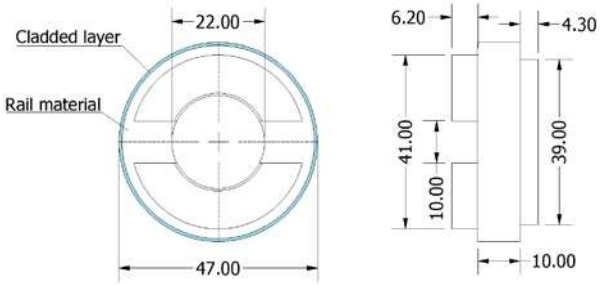

Figure 3 *Cladded rail disc parameters.*

2.2.3. Micro-hardness & Microstructure analysis

For the microhardness mapping and microstructure analysis, the discs were sectioned, mounted in conductive Bakelite base and polished down to a $1\mu m$ Ra finish for the micro-hardness and microstructural analysis. Pre-test micro-hardness measurements were taken with un-tested discs. These results were generated after cladding, but prior to any load application, so did not capture any strain hardening under load. Vickers micro-hardness measurements were taken using a load of 1.00 kg and dwell time of 10 seconds. The indentation process started from the cladding edge towards the centre of the specimen, and the edge was defined as the zero position, see Fig.4.

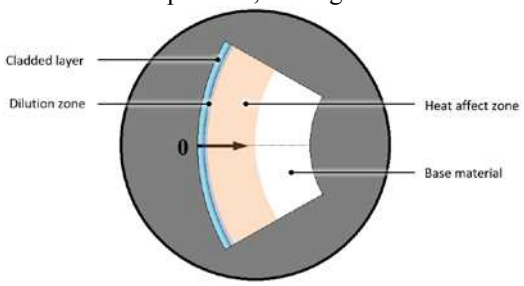

Figure 4 *Hardness mapping direction and location.*

Fig. 5 shows results of microhardness case measurements for the R200 and R260 rail material clad with a single layer of MSS material. As shown in Fig. 5, the hardness of the MSS clad layer ranges from $530HV$ to $630HV$. It can also be seen that the increase of the hardness of the substrate material leads to a corresponding increase in the hardness of the MSS deposit. This will be caused by mixing of the deposit material with the softer or harder substrate during the fusion stage of the cladding process. However, prior to the measurements it was not expected that this mixing effect would extend into the entirety of the clad layer or have such a marked effect.

The material in the "dilution" zone, where the clad material mixed with the base material, has a hardness value between that of the cladded layer and the base material. While in the HAZ, where the base material's microstructure is changed during the heating and cooling process, the hardness reduced gradually towards the boundary with the base material.

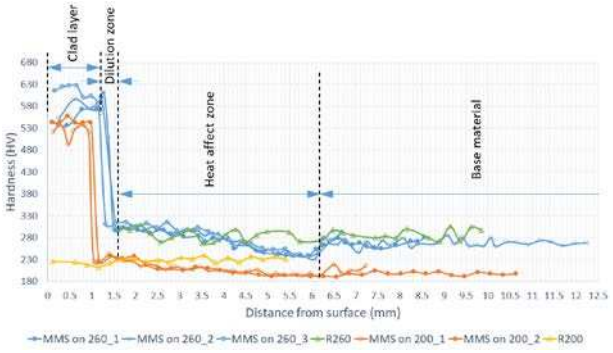

Figure 5 *Hardness mapping for untested samples.*

The microstructure images are shown in Fig. 6 and Fig. 7. These heat affect zones were classified according to the term system of Farichild [21]. The overview images were taken using an optical microscope (CARLZEISS axio imager a2m, Zeiss Göttingen, Germany), and the backscattered electron (BSE) SEM analyse on the HAZ was conducted by using a SEM (Hitachi TM-3030 Tabletop Scanning Electron Microscope, Tokyo, Japan). All the polished specimens for microscope and SEM analysis were etched with 2% Nital solution to expose the grain boundaries.

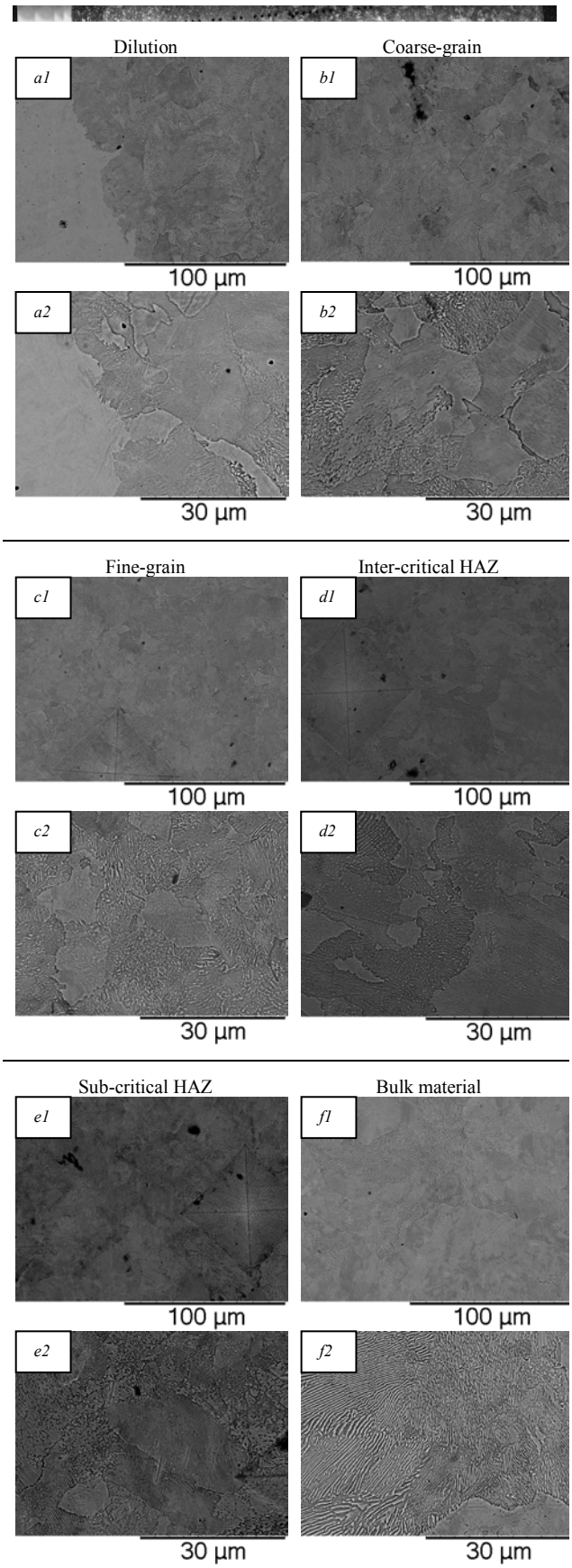

Figure 6 *Microstructure of HAZ in untested MSS on R260 (2% Nital etched): (a1), (a2) are for the Dilution zone. (b1), (b2) are for the Coarse-grain. (c1), (c2) are for the Fine-grain zone. (d1), (d2) are for the Inter-critical zone. (e1), (e2) are for the Sub-critical zone. (f1), (f2) are for the Base material.*

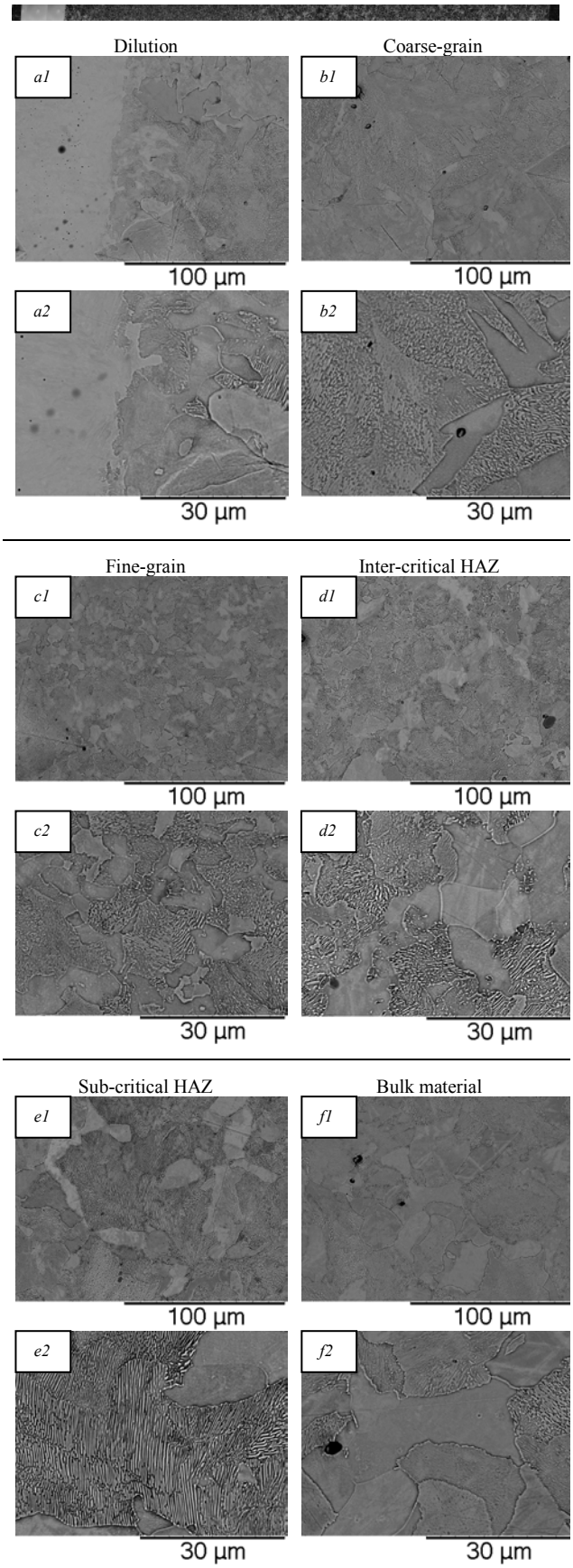

Figure 7 *Microstructure of HAZ in untested MSS on R200 (2% Nital etched): (a1), (a2) are for the Dilution zone. (b1), (b2) are for the Coarse-grain. (c1), (c2) are for the Fine-grain zone. (d1), (d2) are for the Inter-critical zone. (e1), (e2) are for the Sub-critical zone. (f1), (f2) are for the Base material.*

While for the cladded layers, the 2% Nital acid solution could not expose any grain boundaries, therefore a more corrosive solution, 4.76% Nitric, 47.62% hydrochloric and 47.62% water, was used to reveal their microstructure, and the results are shown in Fig. 8 and Fig. 9 for MSS on R260 and MSS on R200, respectively. It should be note that these tiny pores were caused by the strong etchant, as none of them can be observed from the 2% Nital etched samples shown in Fig. 6 and Fig. 7.

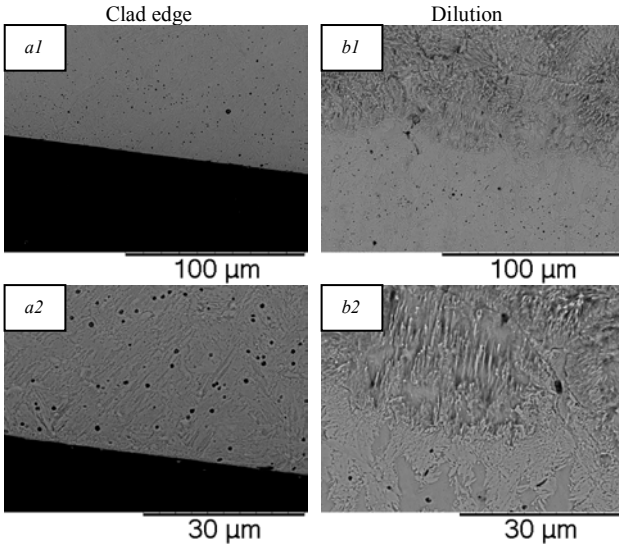

Figure 8 *Microstructure of clad zone in untested MSS on R260 (4.76% Nitric, 47.62% hydrochloric and 47.62% water etched): (a1), (a2) are for the clad edge. (b1), (b2) are for the dilution zone.*

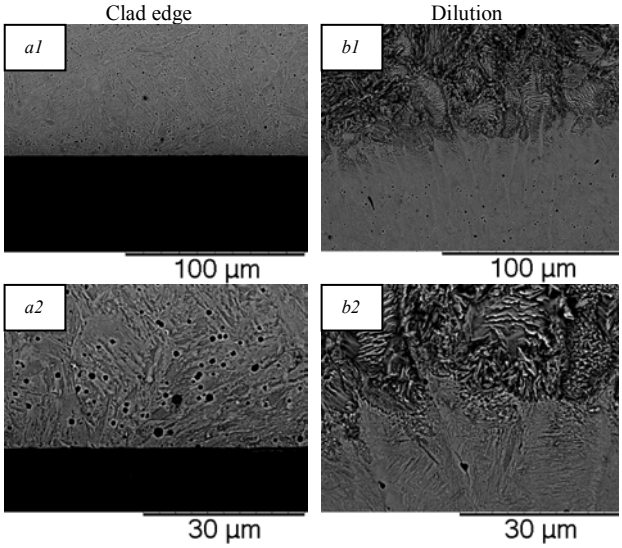

Figure 9 *Microstructure of clad zone in untested MSS on R200 (4.76% Nitric, 47.62% hydrochloric and 47.62% water etched): (a1), (a2) are for the clad edge. (b1), (b2) are for the dilution zone.*

2.3. Tribological testing

Testing was conducted using the SUROS twin-disc testing machine shown in Fig. 1, taking the 47mm diameter wheel and rail discs and loading them to produce a small-scale contact capturing the key elements of combined rolling-sliding behaviour characteristic of a rail-wheel contact. With a line contact length in the lateral dimension of wheel/rail rollers of 10 mm, contact load of 7.14 kN which gives a maximum Hertzian contact pressure of 1500 MPa was used with a rail disc rotational speed of 400 rpm and creep of 1% representing a driving wheel condition. Wear tests were conducted under dry conditions. During the wear testing the tests were stopped every 5,000 cycles so that the evolution of the wear rate could be measured. These are standard wear settings for SUROS testing [19].

Material loss was measured in the tests with microstructural analysis. Microhardness measurements of the specimens was carried out before and after testing to investigate what effect the substrate grade had on the performance of the clad MSS deposit. Comparisons were also made to baseline measurements for R200 and R260.

3. Results and discussion

3.1. Wear results

Figure. 10 shows the evolution of the wear rates of the rail and wheel discs. All tests depicted in this section were conducted under dry contact condition with a maximum Hertzian contact pressure of 1500 MPa and 1% creep. These results were also compared with tests done under identical conditions in [8].

Tests were conducted with the MSS R260 and MSS R200 samples with compressed air jet spraying on samples for temperature control. The results have been compared with the results from Lewis et al. [8], in which tests were done with cooling air. With the cooling air, the contact temperature between discs were kept at 37 ± 1℃ during the whole test.

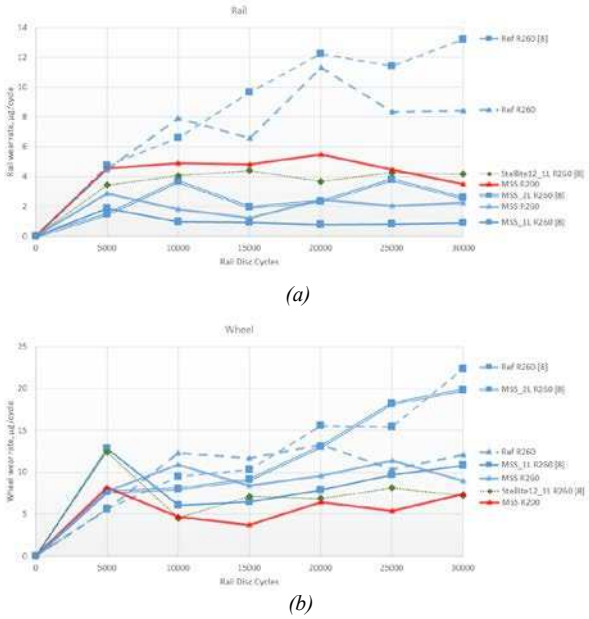

Figure 10 *Wear rate evolution of (a) the rail discs and (b) with the number of test cycles for the R200 clad with MSS and R260 clad with MSS. The chart includes data from [8] with various material deposited onto R260 material. All tests were performed under identical conditions. 1L indicates 1 layer and 2L indicates a 2-layer sample. All samples tested in the work reported in this paper were made with 1 layer.*

From Fig. 10 (a), it can be seen that the MSS on R200 and MSS on R260 rail discs wore at similar rates and had similar performance to an R260 disc clad with

Stellite 12 tested in [8]. As Stellite 12 was seen to be the second best performer of all the deposit materials tested in [8]. It is encouraging that an MSS clad layer on a lower grade of rail steel is still giving a good improvement in wear resistance over the R260 baseline. Even though, as Figure 5 demonstrates, its hardness post cladding, but before load application, was affected. Mechanisms for this will only be revealed, however, once the tested samples are sectioned and case hardness measurements performed. Interestingly the post-test surface hardness of the MSS 1L tested in [8] was 766HV compared to 630 HV for the MSS clad on R260 sample tested here (see Figure 5). This indicates that it could be inferred that a significant degree of work hardening may have occurred during the tests performed in this research. It must also be noted though that the 1 layer samples tested in this work wore more severely than the 1 layer MSS sample tested in [8]. There are a few potential explanations for this: a) that the powder and hence the eventual deposited MSS was from a different batch for the tests reporting in this paper as compared to the samples in [8]. Also in this work whole cylinders of R200 and R260 material were clad and then manufactured into SUROS samples. In [8] the SUROS samples were first machined and then individually clad. This latter approach caused issues with heat dissipation during the cladding process and very high cooling rates of the clad were observed.

Table. 3 summarises the wear rate of all the rail specimens shown in Figure 10 averaged over the whole 30,000 cycle test period. The average for the MSS clad on 200 is distorted by the wear rate at 25,000 cycles. Otherwise it is only slightly above MSS on R260. In Table. 3 any wear rate which was in excess of either the Reference (R260 Grade) wheel or rail, i.e. 100% or greater, has been highlighted red. Any wear rate which is less than the reference is highlighted green indicating good wear performance. Wear rates which are less than 50% of the reference case are highlighted light green indicating superior wear performance.

It should be noted that the wear rates of the tests in [8] were slightly higher (both wheel and rail around 20%) than the current tests, when comparing the results of reference R260 tests. It can be seen from Table. 3 that all of the clad rail discs tested are in the good/ superior wear category. The MSS on R260 rail discs have shown superior wear resistance, which gave a 65%-73% wear rate reduction. Even the MSS on R200 rail discs have presented a 40% wear rate reduction compared to the standard R260 samples. At the same time, the wear rate of corresponding wheel discs also fell within the good wear category.

Table 3 *Averaged wear rates of rail specimens over the entire 30,000 cycles (Data from similar tests performed in [8] included for comparison).*

	Wear Rate		**Wear Rate**	
	$\mu g/cycle$		**Percentage of Ref R260**	
Clad	**W**	**R**	**W**	**R**
Ref R260	10.88	7.84	100%	100%
Ref R260 [8]	13.14	9.64	121%	123%
MSS R200	5.97	4.62	55%	59%
MSS R260	9.49	2.11	87%	27%
MSS_1L R260 [8]	8.96	1.04	82%	13%
MSS_2L R260 [8]	12.65	2.63	116%	34%
Stellite12_1L R260 [8]	7.72	4	71%	51%

3.2. Traction

Table 4 shows average traction results for each of the different claddings compared to an unclad reference R260 grade rail disc.

Table 4 *Traction coefficient comparison with results from [8].*

Ref R260	Ref R260 [8]	MSS R200	MSS R260	MSS_ 1L R260 [8]	MSS_ 2L R260 [8]	Stellite 12_1L R260 [8]
0.37	0.39	0.36	0.38	0.395	0.385	0.405

It can be observed that the cladded samples had a similar traction coefficient with the ref R260 samples, which suggests the cladded layer does not influence the traction properties of rail.

3.3. Topography measurements

All surfaces were examined using the optical (non-contact) Alicona Infinite-Focus SL profilometer (Alicona Imagine GmbH, Raaba, Austria) after 30000 cycles, producing high-resolution images and 3D surface profiles measurements with a vertical resolution of up to 10 nm.

Table 5 *Traction coefficient comparison with results from [8].*

Ref 260 without cladding	**MSS cladding on R260**	**MSS cladding on R200**
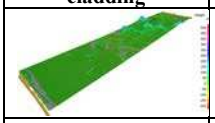	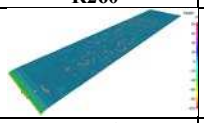	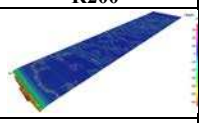
Ra: 6.0614μm Rq: 18.6459μm Rz: 71.4973μm	Ra: 0.6450μm Rq: 0.8080μm Rz: 3.4856μm	Ra: 0.7464μm Rq: 0.9542μm Rz: 4.1182μm

As can be seen from Table. 5, both MSS on R260 and MSS on R200 specimens have shown a smooth surface finish after tests, with a surface roughness $R_a < 0.75\mu m$. This indicates that only mild wear occurred during tests, and these smooth surfaces show no sign of flake formation characteristic of a significant depth of material reaching the ductility exhaustion strain at which large flakes would form. In contract, on the reference R260 rail disc it can be observed that the top layer of material was peeling up from the surfaces, and the surface roughness was 10 times higher than that of the cladded specimens. This suggests that strain in the surface has accumulated (i.e. by a ratchetting mechanism) to the point of ductility exhaustion at which

it loses integrity and breaks away from the main body of the steel.

3.4. Sub-surfaces inspection

After the surface topography measurements, tested rail specimens were then sectioned and examined for: micro hardness and micro- structural changes. Fig. 11 gives a comparison of the hardness pier and after the test. It should be noted that these hardness values were gathered from different specimens, but all were taken from the same parent material.

As can be seen from Fig. 11 (a), the outside layer of material has worked hardened after testing, and a hardness of around 480 HV was achieved near the top surface of the tested specimen. While for the cladded rail specimens, the work-hardened effects were not as marked as for the reference R260 sample as shown in Fig. 11 (b) and Fig. 11 (c).

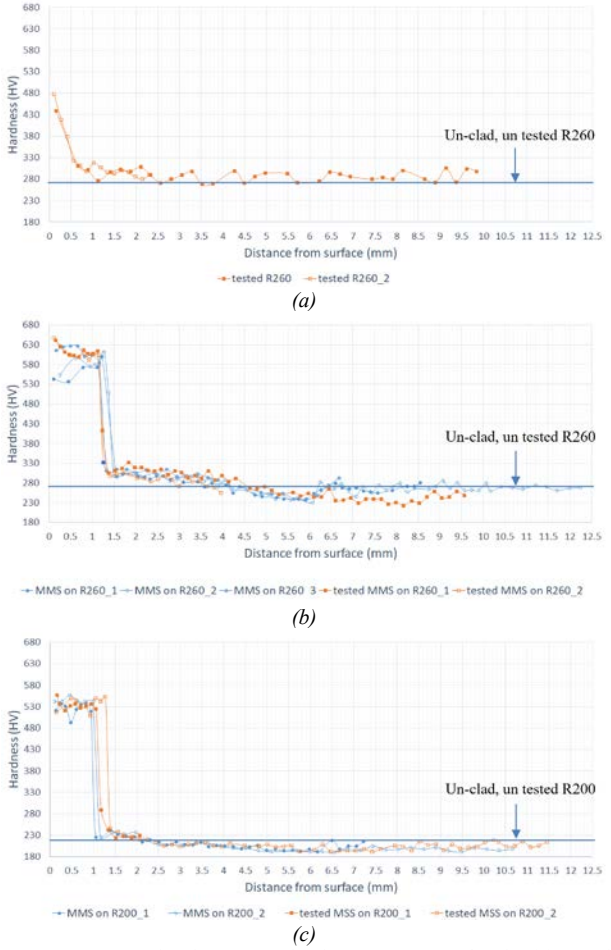

Figure 11 *Microhardness case depth measurements for the (a) tested reference R260 sample (b) MSS clad on R260 and (c) MSS clad on R200 with the straight line representing the mean microhardness of standard un-clad, un-tested rail material. All measurements were performed with a load of 1kg.*

The sub-section of samples was also examined under SEM to check the plastic deformation depth caused by testing. According to measurements judged by visually observation, see Fig. 12 (a), the R260 samples had a plastic deformation depth of approximately $400\,\mu m$ while the clad rail samples only had $10-20\,\mu m$. As shown in Fig. 12 (b), only a very thin layer of the MSS clad layer shows material flow, and no cracks could be observed within this deformation layer, i.e. the material had not reached its ratchetting strain ductility exhaustion strain. The rest of the clad layer had the same structure as the untested samples shown in Fig.7 and Fig. 8. The low amount of plastic deformation in the clad rail specimens also explains why no cracks were seen in all of the clad rail specimens.

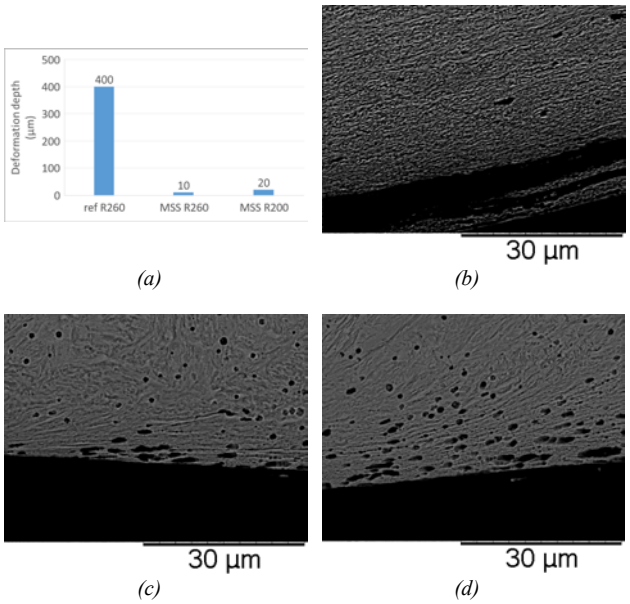

Figure 12 *(a) plastic deformation depth comparison and clad edge's microstructure deformation of tested samples: (b) is the Reference R260 sample without cladding. (c) and (d) are the clad edge of MSS on R260 and MSS on R200 samples, respectively. All samples were tested under 1500 MPa contact pressure, and 1% slip ratio with cooling air.*

4. Conclusions

Twin-disc tests have been performed on both R200 and R260 rail after being laser clad with a single layer of MSS material. It has been shown that:

- MSS can be successfully deposited on a R200 grade of rail material which is softer than previously the used R260.
- A sample with the softer R200 substrate material also showed a corresponding reduction in the hardness of the clad layer relative to the R260 substrate. Additional tests are needed to isolate the cause, which may be due to mixing of the softer/harder substrate material with the clad layer, but could also be influenced by the different thermal route taken in preparing the samples.
- The hardness differential between the clad R200 and R260 is reflected in the wear rates between the two samples with the R200 clad sample giving a higher wear rate.
- Despite differences between clads on R200 and R260 both samples wore below $5\mu g/cycle$. This represents a wear rate of 50% or less relative to the reference R260 sample without cladding.

Although cladding on a lesser grade of rail does have an effect on the hardness and wear performance of the clad layer, the resulting wear performance of the clad layer assessed using the twin disc approach is still improved, with the wear rate reduced to 0.59 times of the R260 material alone. R260 material alone. In addition, the minimum plastic deformation depth and the smooth surface finish after tests indicates the clad rail specimen are also beneficial for wear rate reduction of the untreated wheel.

Acknowledgments
The authors would like to acknowledge ESPRC and Rail Safety and Standards Board (RSSB) who provided equal joint funding to support this work (Project no. EP/M023044/1).

References

[1] R. Lewis and U. Olofsson, "Mapping rail wear regimes and transitions," Wear, vol. 257, no. 7, pp. 721-729, 2004/10/01/ 2004.
[2] G. Donzella, M. Faccoli, A. Ghidini, A. Mazzù, and R. Roberti, "The competitive role of wear and RCF in a rail steel," Engineering Fracture Mechanics, vol. 72, no. 2, pp. 287-308, 2005/01/01/ 2005.
[3] I. Guideline, "Definitive guidelines on the use of different rail grades," Deliverable report D, vol. 4, 2006.
[4] W. J. Wang, J. Guo, Q. Y. Liu, M. H. Zhu, and Z. R. Zhou, "Study on relationship between oblique fatigue crack and rail wear in curve track and prevention," Wear, vol. 267, no. 1, pp. 540-544, 2009/06/15/ 2009.
[5] S. Niederhauser and B. Karlsson, "Fatigue behaviour of Co–Cr laser cladded steel plates for railway applications," Wear, vol. 258, no. 7, pp. 1156-1164, 2005/03/01/ 2005.
[6] W. J. Wang, J. Guo, Q. Y. Liu, and M. H. Zhu, "Effect of laser quenching on wear and damage of heavy-haul wheel/rail materials," Proceedings of the Institution of Mechanical Engineers, Part J: Journal of Engineering Tribology, vol. 228, no. 1, pp. 114-122, 2014/01/01 2013.
[7] W. J. Wang, J. Hu, J. Guo, Q. Y. Liu, and M. H. Zhu, "Effect of laser cladding on wear and damage behaviors of heavy-haul wheel/rail materials," Wear, vol. 311, no. 1, pp. 130-136, 2014/03/15/ 2014.
[8] S. R. Lewis et al., "Improving rail wear and RCF performance using laser cladding," Wear, vol. 366-367, pp. 268-278, 2016/11/15/ 2016.
[9] S. Jalili Hassankiadeh, "Failure analysis of railway switches and crossings for the purpose of preventive maintenance," ed, 2011.
[10] W.-J. Zwanenburg, "Modelling degradation processes of switches & crossings for maintenance & renewal planning on the Swiss railway network," 2009.
[11] C. Guo et al., "Effects of WC–Ni content on microstructure and wear resistance of laser cladding Ni-based alloys coating," Surface and Coatings Technology, vol. 206, no. 8, pp. 2064-2071, 2012/01/15/ 2012.
[12] H.-m. Guo, Q. Wang, W.-j. Wang, J. Guo, Q.-y. Liu, and M.-h. Zhu, "Investigation on wear and damage performance of laser cladding Co-based alloy on single wheel or rail material," Wear, vol. 328-329, pp. 329-337, 2015/04/15/ 2015.
[13] W. J. Wang, Z. K. Fu, X. Cao, J. Guo, Q. Y. Liu, and M. H. Zhu, "The role of lanthanum oxide on wear and contact fatigue damage resistance of laser cladding Fe-based alloy coating under oil lubrication condition," Tribology International, vol. 94, pp. 470-478, 2016/02/01/ 2016.
[14] S. R. Lewis et al., "Full-scale testing of laser clad railway track; Case study – Testing for wear, bend fatigue and insulated block joint lipping integrity," Wear, vol. 376-377, pp. 1930-1937, 2017/04/15/ 2017.
[15] Z. K. Fu, H. H. Ding, W. J. Wang, Q. Y. Liu, J. Guo, and M. H. Zhu, "Investigation on microstructure and wear characteristic of laser cladding Fe-based alloy on wheel/rail materials," Wear, vol. 330-331, pp. 592-599, 2015/05/01/ 2015.
[16] S. R. Lewis, R. Lewis, and D. I. Fletcher, "Assessment of laser cladding as an option for repairing/enhancing rails," Wear, vol. 330-331, pp. 581-591, 2015/05/01/ 2015.
[17] J.-M. Chen, C. Guo, and J.-S. Zhou, "Microstructure and tribological properties of laser cladding Fe-based coating on pure Ti substrate," Transactions of Nonferrous Metals Society of China, vol. 22, no. 9, pp. 2171-2178, 2012/09/01/ 2012.
[18] P. Beaty, B. Temple, M. B. Marshall, and R. Lewis, "Experimental modelling of lipping in insulated rail joints and investigation of rail head material improvements," Proceedings of the Institution of Mechanical Engineers, Part F: Journal of Rail and Rapid Transit, vol. 230, no. 4, pp. 1375-1387, 2016/05/01 2015.
[19] D. Fletcher and J. Beynon, "Development of a Machine for Closely Controlled Rolling Contact Fatigue and Wear Testing," 2000.
[20] B. Dahl, B. Mogard, B. Gretoft, and B. Ulander, "Repair of rails on-site by welding," Swedish National Rail, SE-781, vol. 85, 1995.
[21] D. Farichild, N. Bangaru, J. Koo, P. Harrison, and A. Ozekcin, "A study concerning intercritical HAZ microstructure and toughness in HSLA steels," Welding Journal, vol. 70, no. 12, pp. 321. s-329. s, 1991.